International Journal of Technical Research and Applications e-ISSN: 2320-8163,
www.ijtra.com Volume 2, Issue 4 (July-Aug 2014), PP. 44-48

A HYBRID APPROACH OF WAVELETS FOR EFFECTIVE IMAGE FUSION FOR MULTIMODAL MEDICAL IMAGES

RENUKA DHAWAN[1], NARESH KUMAR GARG[2]
Department of Computer Science,
PTU GZS Campus,
Bathinda, India

***ABSTRACT*: Image fusion is a technique used to integrate a high-resolution panchromatic image with multispectral low-resolution image to produce a multispectral high-resolution image, that contains both the spatial information of the panchromatic high-resolution image and the color information of the multispectral image .Although an increasing number of high-resolution images are available along with sensor technology development, the process of image fusion is still a popular and important method to interpret the image data for obtaining a more suitable image for a variety of applications, like visual interpretation and digital classification. To get the complete information from the single image we need to have a method to fuse the images. In the current paper we are going to propose a method that uses hybrid of wavelets for Image fusion**.

Keywords: **Image fusion, Wavelet Transform, MFHWT, BIOR Wavelet.**

1. INTRODUCTION

The objective of image fusion is to combine complementary as well as redundant information from many images to have a fused resultant image. Thus, the resultant image produced must contain a more accurate details of the scene than any of the individual sources image and is more beneficial for human visual and for machine perception or even further image processing and analysis tasks[2]. Depending on the applications, fusion problems can occur in different situations, in which the types of information elements are not the same. The main fusion situations in image processing are the following:-

A. Several images from the same sensor.

This consists, for example, of several channels on the same satellite, or multi-echo images in MRI, or also of image sequences for scenes in motion. The data in those cases is relatively homogenous because it corresponds to similar physical measurements.

B. Several images from different sensors:-

This is the most common case, in which the different physical principles of each sensor allow the user to have complementary perspectives of the scene [4]. They can consist of ERS and SPOT images, MRI or ultrasound images, etc. The heterogeneity is then much greater, since the various sensors do not deal with the same aspects of the phenomenon. Each image gives a partial image with no information on the characteristics they are not meant to observe (for example, an anatomical MRI yields no functional information and the resolution of a PET scan is too low for a precise view of the anatomy).

C. Several elements of information extracted from a same image:-

In this situation, different types of information are extracted from an image using several sensors, operators, classifiers, etc., that rely on different characteristics of the data and attempt to extract different objects, often leading to very heterogeneous elements of information to fuse. The extracted information can involve the same object (fusion of contour detectors, for example) or different objects and the goal is then to find an overall interpretation of the scene and consistency between the objects. The elements of information can be on different levels (very local, or more structural when studying spatial relations between objects).

D. Images and another source of information:-

By another source of information, we mean, for example, a model, which may be particular like a map, or generic like an anatomical atlas, a knowledge base, rules, information provided by experts, etc [13]. The elements of information are again in very different forms, both in nature and in their initial representation (images in the case of a map or a digital atlas, but also linguistic descriptions, databases, etc.).

II. WAVELET METHODS FOR IMAGE FUSION

In the wavelet domain, high-frequency detail coefficients have large absolute values correspond to sharp intensity changes and present salient features in the image whereas edges, lines and region boundary present. Low-frequency approximation coefficients are coarse representations of the original image and may have inherited some properties such as the mean intensity or texture information of our original image. As an approximation sub-image and detail sub-images have different physical meaning, they are treated differently in the fusion process. In this, low-frequency detail of the sub-images, and denotes the approximate components of input images; and we use image energy as weight coefficient to fuse them. Let $W_{A\varphi}$ denote the low-frequency detail of the sub-image of input source image A. The energy of $W_{A\varphi}$ is denoted by $EW_{A\varphi}$:

$$EW_{A\varphi} = \sum_{m=1}^{M}\sum_{n=1}^{N}\frac{\left(W_{A\varphi}(m,n)\right)2}{M \times N} \quad [5] \quad (1)$$

And let $W_{B\varphi}$ denote the low-frequency detail sub-image of input source image B, its energy is $EW_{B\varphi}$:

$$EW_{B\varphi} = \sum_{m=1}^{M} \sum_{n=1}^{N} \frac{\left(W_{B\varphi}(m,n)\right)2}{M \times N} \quad [5]$$

Let FW_{φ}be the low frequency approximate sub image of the fused image. The fusion rule is as written:

$$FW_{\varphi}(m,n) = \frac{EW_{A\varphi}}{EW_{A\varphi}+EW_{B\varphi}} W_{A\varphi}(m,n) + \frac{EW_{B\varphi}}{EW_{A\varphi}+EW_{B\varphi}} WB\varphi(m,n)$$

To the high frequency sub-images, we will use local gradient algorithm to fuse detail images because derivatives have a stronger response to fine detail. The most simplest derivative operator is the Laplacian, which, for a function (image) *f*(*x*, *y*) of two variables, is defined as:

$$\nabla^2 f = \frac{\partial^2 t}{\partial x^2} + \frac{\partial^2 f}{\partial y^2}$$

Denote $\boldsymbol{W}^{i}_{A\varphi}(\mathrm{m,n}),\ \mathrm{i = H,V,D}$ and $1 \le \mathrm{m} \ge \mathrm{M},\ 1 \le \mathrm{n} \ge \mathrm{N}$, the three high frequency detail subimages of input mid-wave infrared image, and then the gradients of our three sub images are $\nabla^2 \boldsymbol{W}^{i}_{A\varphi}(m,n),\ \ i = H,V,D.$ and the gradients of the input long wave infrared image are $\nabla^2 \boldsymbol{W}^{i}_{B\varphi}(m,n),\ \ i = H,V,D.$

Let $FW\varphi i(m,n)\,, i = H,V,D$ be the fused high frequency components, as they are defined as

$$FW^{i}_{\varphi}(m,n) = \begin{cases} W^{i}_{A\varphi}(m,n)\,, if\ \left|\nabla^2 \boldsymbol{W}^{i}_{A\varphi}(m,n)\right| \ge \left|\nabla^2 \boldsymbol{W}^{i}_{A\varphi}(m,n)\right| \\ W^{i}_{B\varphi}(m,n)\,, if\ \left|\nabla^2 \boldsymbol{W}^{i}_{A\varphi}(m,n)\right| < \left|\nabla^2 \boldsymbol{W}^{i}_{A\varphi}(m,n)\right| \end{cases}$$

[8]

At decomposition level we can use modified fast haar wavelet transformation In case of HAAR: *Haar Wavelets.* The Haar wavelet is the simplest and oldest one. It is a step function taking values 1 and -1. Its scaling function can be expressed as following: $\varphi(t) = 1 \quad ; 0 \le t < 1$

$\varphi(t) = 0$;otherwise

$\Psi(t) = 0 \quad ; 0 \le t < ½$

$(t) = 1 \quad ; \frac{1}{2} \le t < 1$

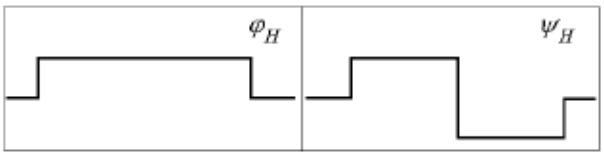

[12]

Fig.1 Haar scaling function (left) and Haar mother wavelet (right)

Decompose the image using wavelet (Sub band) with MFHWT: Modified Fast Haar Wavelet Transform: In MFHWT, first average the sub signal (a' =a1,a2, a3… $a_{n/2}$), at one level for a signal of length N i.e. f =(f1, f2,f3,f4…fn) is

$$a_m = \frac{f_{4m-3} + f_{4m-2} + f_{4m-1} + f_{4m}}{4},\ m = 1,2,3,\ldots,N/4,$$

[2]

and first detail sub-signal(d'= $d_1,d_2,d_3\ldots.d_n$), at the same level is given as :

$$d_m = \begin{cases} \dfrac{(f_{4m-3} + f_{4m-2}) - (f_{4m-1} + f_{4m})}{4},\ m = 1,2,3,\ldots,N/4, \\ 0 \qquad\qquad\qquad\qquad ,\ m = N/2,\ldots,N. \end{cases}$$

For the orthogonal wavelets the reconstruction formula and the decomposition Formula coincides. A biorthogonal wavelets system consists of two sets of wavelets generated by a mother wavelet ψ and a dual wavelet $\psi\tilde{}$, for
which

(ψ˜k,,ψm,n) = δk,mδ_,n, for all integer values *k, _,m* en *n*.

We assume that *(ψk,)* constitute a so called Riesz basis (numerically stable) of *L2(*IR*)*, i.e. *A (f, f) ≤ __k,_ ξk,__2 ≤ B (f, f)*
for positive constants *A* en *B*, where *f = _k,_ ξk,_ψk,_*.

THE RECONSTRUCTION FORMULA NOW READS *F =_K,(F,ΨK,_)Ψ˜K,_*

III. PROPOSED TECHNIQUE

The methodology of work will start with the overview of image fusion algorithms. The results of various algorithms will be interpreted on the basis of different quality measures. Thus, the methodology for implementing the objectives can be summarized as follows:-

1 To focus on the feature detection so that we decide which algorithm to be applied.

2 Based on the Detection we will apply the hybrid wavelet transform based on RMFHWT and Bior transform for Image Fusion.

3 This will increase the efficiency of the fusion method and quality in the Image.

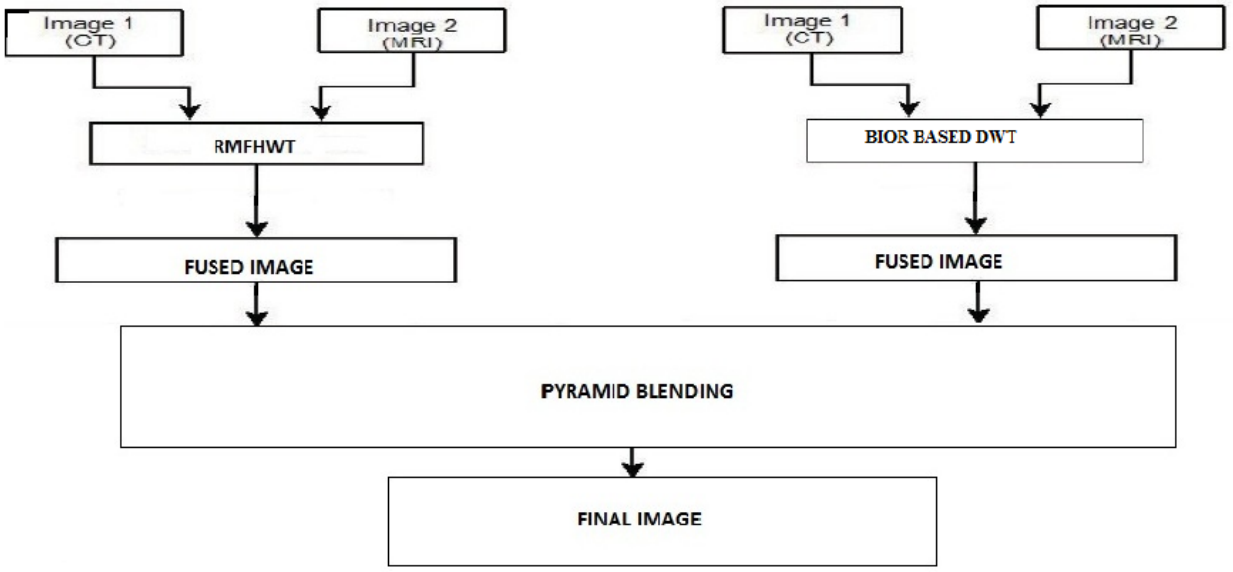

Fig.2. Overview of Hybrid Technology of Image Fusion Consists of RMFHWT and Bior Based Dwt

IV. QUALITY METRICS

The performance, experimental results or comparison of the proposed scheme is evaluated by various quantitative measures like:

A. Entropy:

Entropy is one of the quantitative measures in digital image processing. Claude Shannon introduced the entropy concept in quantification of information content of the messages. Although he used entropy in communication, it can be also used as a measure and also quantifying the information content of the digital images. Any digital image consists of the pixels arranged in several rows and many columns [9]. Every pixel is defined by its position and also by its grey scale levels. For an image which is having L grey levels, the entropy is defined as:

$$H = -\sum_{i=1}^{L} P(i) \log_2 P(i)$$

H-Pixel entropy;
L-image's total grayscale;

Where $P_i = N_i/N_p = \{p_0, p_1 \dots p_{i\dots\dots} p_{l-1}\}$ reflects the probability distribution which has different gray values in the image. The diagram of $i - N_i$ is the Image's gray histogram. The entropy of fusion image is larger which is respected that the amount information of fused images is increased, the Information which is contained in fusion images is richer and fusion quality is better. Where is the probability (here frequency) of each grey scale level.

For images with high information content the entropy will be large. The larger alternations and changes in an image give larger entropy and the sharp and focused images have more changes than blurred and miss focused images.[1] Hence, the entropy is a measure to assess the quality of different aligned images from the same scene.

B. Quality

The overall quality of images can be measured by using the brightness μ, contrastσand sharpness S. The following criteria are used for brightness, contrast and the sharpness [3].

i. Let μ_n be the normalized brightness parameter, such that

$$\mu_n = \begin{cases} \mu/225 & \mu < 154 \\ 1 - \mu/225 & otherwise \end{cases}$$

eq(1.2) [14]

A region is considered to have sufficient brightness when $0.4 \leq \mu_n \leq 0.6$

ii. Let σ_n be the normalized contrast parameter, such that

$$\sigma_n = \begin{cases} \sigma/128 & \mu \leq 64 \\ 1 - \sigma/128 & otherwise \end{cases}$$

A region is considered to have sufficient contrast when $0.25 \leq \sigma_n \leq 0.5$. When $\sigma_n \leq 0.25$, the region has poor contrast, and when $\sigma_n > 0.5$, the region has too much contrast.

Let S_n be the normalized sharpness parameter, such that S= *min* (2.0, *S*/100). When$S_n > 0.8$, the region has sufficient sharpness. The image quality is assessed using

$$Q = 0.5\mu_n + \sigma_n + 0.1S_n \qquad \text{eq(1.4)}$$

Where 0 <*Q* <1.0 is the quality factor. A region is classified as good when *Q* > 0.55, and poor when $\sigma_n \leq 0.5$[11]. An image I classified as good when the total number of regions that are classified as good exceeds.

C. Standard Deviation:

Standard deviation is usually used to represent the deviation degree of the estimation and the average of the random variable [18]. The standard deviation mainly reflects the discrete degree between the pixel gray and the mean value. The bigger the standard deviation is, the more discrete will be the distribution of gray levels. It estimates the activity level as follows:

$$A_l(p) = \sum_{scS,tcT} \left(\frac{|D_l(m+s,n+t,j,k) - D_l(m+s,n+t,j,k)|^2}{S \times T} \right)^{\frac{1}{2}}$$

eq(1.5) [6]

Where, S and *T*are sets of the current window.

D. Peak Signal to Noise Ratio (PSNR) & Mean Square Error (MSE): -

Image quality assessment is an important issue in image fusion. MSE used to measure the degree of image distortion because they can represent the overall gray-value error contained in the whole image, and is mathematically tractable as well[3]. In many applications, it is usually straightforward to design systems that minimize MSE. MSE works satisfactorily when the distortion is mainly caused by contamination of additive noise.

The PSNR computes the peak signal-to-noise ratio between two images (in decibels). This computed ratio is often used as a measure of quality between the original and the compressed image. The higher the PSNR, higher will be the quality of reconstructed image.

The *Mean Square Error (MSE)* and the *Peak Signal to Noise Ratio (PSNR)* are the two metrics of error are used to compare quality of compressed image. The MSE also displays the cumulative squared error between the two images, compressed and the original image [15], on the other hand, the PSNR represents peak error. If value of MSE is low, the lower is the error.

To compute the PSNR, We must calculate the mean-squared error with the help of equation:

$$MSE = \frac{\sum_{M,N} [I_1(m,n) - I_2(m,n)]^2}{M * N}$$

In the above equation, *M* and *N* are the number of rows and columns in the images, respectively. Then the block will compute the PSNR using the equation:

$$PSNR = 10\log_{10}\left(\frac{R^2}{MSE}\right)$$ [5]

In the previous equation, *R* is the maximum fluctuation in our input image data type. We can say, if our input image is having a double-precision floating-point data type, then value of R is 1. And if it having an 8-bit unsigned integer data type that is, *R* is 255, etc.

V. MODIFIED FAST HAAR WAVELET TRANSFORM

In MFHWT, first average sub signal (a' =a1, a2, a3… an/2), at one level for a signal of length N i.e. f = (f1, f2, f3, f4…fn) is

$$a_m = \frac{f_{4m-3} + f_{4m-2} + f_{4m-1} + f_{4m}}{4}, \quad m = 1, 2, 3, \ldots, N/4,$$

[12]

and first detail sub-signal(d'= d1,d2,d3….dn), is given as(at the same level):

$$d_m = \begin{cases} \dfrac{(f_{4m-3} + f_{4m-2}) - (f_{4m-1} + f_{4m})}{4}, & m = 1, 2, 3, \ldots, N/4, \\ 0, & m = N/2, \ldots, N. \end{cases}$$

[12]

In this four nodes are considered two nodes as in HT and FHT. The MFHWT is faster in comparison to FHT and reduces the calculation work. In MFHWT, we get the values of approximation and detail coefficients one level ahead than the FHT and HT [1].

VI. BIORTHOGONAL WAVELET

Biorthogonal wavelets provide a pair of scaling functions and associated scaling filters, one for analysis and one for synthesis. Similarly, there is also a pair of wavelets and associated wavelet filters one for analysis and one for synthesis. This family of wavelets exhibits the property of linear phase, which is needed for signal and image reconstruction. There are different numbers of vanishing moments and regularity properties for the analysis and synthesis wavelets. In this, we can use the wavelet with the greater number of vanishing moments for analysis whiles the smoother wavelet for reconstruction [1]. Therefore, here we can use two wavelets, one for decomposition (on the left side) and the other for reconstruction (on the right side) instead of the same single one.

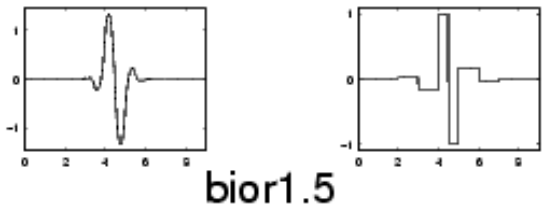

[1]

Fig 3. Bior Wavelet

VII. RESULTS

To illustrate the effectiveness of algorithm proposed, we are taking four quality metrics and the outcome is compared with the previous algorithms. These are: Entropy, PSNR (peak to signal noise ratio), Standard Deviation and Quality.

TABLE I COMPARATIVE RESULTS OF ALGORITHM: ENTROPY, PSNR (PEAK TO SIGNAL NOISE RATIO), QUALITY AND SD (STANDARD DEVIATION). THE FOCUS IS SET ON TO HAVE COMPARATIVELY GOOD MEASURES OF THESE PARAMETERS

IMAGE SET	Entropy		PSNR		S.D		Quality Index	
	Earlier Technique	Proposed Technique	Earlier Technique	Proposed Technique	Earlier Technique	Proposed Technique	Earlier Technique	Proposed Technique
CT1,MRI1	5.06	6.9	19.5	45.4	9.3	69.5	27.5	167.3

CT2,MRI2	4.9	7.2	22.94	37.4	12.8	79.23	22.67	136.8
MRI3,MR14	5.2	6.8	11.9	51.02	11.5	43.6	26.9	166.9

VIII. CONCLUSION AND FUTURE SCOPE

In the current paper we have given the comparison of hybrid wavelet MFHWT and BIOR, with redundant discrete wavelet transformation. Quality Metrics have been used for computing results to compare quantitatively these techniques. Experimental results show that proposed method achieves well than the prior methods (RDWT) in terms of quality of images. The proposed method increases the quality significantly, while preserving the important details or features. This also gives the better results in terms of visual quality. For future work, the other hybrids of Curve let and contourlet transformation may be done to improve the results. This algorithm can be used in other type of images like Remote sensing images, Ultrasound images, SAR images etc. Other quality metrics can be used to judge the performance of this algorithm. And further improvements can also be done in the algorithm to improve the quality.

REFERENCES

[1] Chandra Prakash, S Rajkumar and P.V.S.S.R. Chandra Mouli" Medical Image Fusion Based on Redundancy DWT and Mamdani Type Min-sum Mean-of-max Techniques with Quantitative Analysis" May, 2012 Page No. 978-1-4673-0255.

[2] Renuka Dhawan, "A comprehensive review of different techniques of image fusion", International Journal of Engineering and Computer Science ISSN: 2319-7242, Volume 3 Issue 3 March, 2014 Page No. 5098-5101.

[3] Pohl, J van Genderen, "Multi-sensor Image Fusion of remotely sensed data: concepts, methods and applications", International Journal Remote Sensing ISSN: 345-360, volume 19 (5) March 2009 Page No. 567-589.

[4] Mitianoudis. N. and T. Stathaki, "Pixel-based and region-based image fusion schemes using ICA bases," IEEE Transactions on Geoscience and Remote Sensing, volume. 8, no. 2, June 2007, Page No. 131–142.

[5] S. T. Li, J. T. Kwok, Y. N. Wang, "Multi focus image fusion using artificial neural networks", Pattern Recognition Letters, volume. 23, no. 8, August 2012, Page No. 985–997.

[6] S.Udomhunsakul, and P. Wongsita, "Feature extraction in medical MRI images", Proceeding of 2004 IEEE Conference on Cybernetics and Intelligent Systems, volume.1, December. 2004, Page No. 340- 344.

[7] Li H., Manjunath B.S. And Mitra, S. K "Multi-sensor image fusion using the wavelet Transform", Graphical Models and Image Processing, volume 57(3), September 1995, Page No. 235-245.

[8] Tang, G. and Pu, J, "Image Fusion Based on Multi-wavelet Transform", Proceedings of the 2006 IEEE International Conference on Mechatronics and Automation, June 25- 28, 2006, Luoyang, China, Page No.25-28.

[9] Wu, K .Wang, C .and Li, L. (2010), "Image Fusion at Pixel Level Algorithm Is Introduced and the Evaluation criteria", International Conference on Educational and Network Technology (ICENT 2010), Page No.585-588.

[10] Hu, X. Lu, H and Zhang, LA "New Type of Multi-focus Image Fusion Method Based on Curvelet Transforms", International Conference on Electrical and Control Engineering, August 2010 Page No. 172 -175.

[11] Kor S. and Tiwary U., " Feature Level Fusion of Multimodal Medical Images in Lifting Wavelet Transform Domain", Proceedings of the 26th Annual International Conference of the IEEE EMBS San Francisco, 2004 IEEE , Page No. 1479-1482.

[12] Chitroub S., 2010. "Classifier combination and score level fusion: concepts and practical aspects". International Journal of Image and Data Fusion, Volume. 1, No. 2, June 2010, pp. 113–135.

[13] Shu Xia, Z .and Xun Zhang, C. , "Medical Image Fusion Based on An Improved Wavelet Coefficient Contrast", School of Computer Science, Shaanxi Normal University, October 2009, China, Page No..1-4.

[14] Kavitha C T, Chellamuthu C, Rajesh R "Medical image fusion using integer wavelet transform and pulse -coupled neural network", Proceedings of 2011 IEEE International Conference on Computational Intelligence and Computing Research 2011; Page No..834-838.

[15] Sun, F. Li, S .and Yang, B."A New Color Image Fusion Method for Visible and Infrared Images", Proceedings of IEEE International Conference on Robotics and Biometrics Sanya, June 2008, China, Page No.. 2043 -2048.

[16] Mallat,S.G. "A theory of multiresolution signal decomposition: the wavelet representation", IEEE Trans on Pattern Analysis and Machine Intelligence,volume.11,July 1989, Page No.674-693.

[17] Ali, F.E .Dokany, I. M. El.Saad, A. A. And Abd El-Samie, F.E."Fusion of MR and CT Images Using The Curvelet Transform", 25th National Radio Science Conference (NRSC 2008).

[18] Burt, P. "A gradient pyramid basis for pattern selective image fusion.", the Society for Information Displays (SID) International Symposium Digest of Technical Papers, 23, January 1993, Page No. 467-470.